



Cite this: *Nanoscale*, 2017, 9, 4430

## Integration of stem cell-derived exosomes with *in situ* hydrogel glue as a promising tissue patch for articular cartilage regeneration†

Xiaolin Liu,<sup>‡a</sup> Yunlong Yang,<sup>‡a,b</sup> Yan Li,<sup>b</sup> Xin Niu,<sup>a</sup> Bizeng Zhao,<sup>a</sup> Yang Wang,<sup>\*a</sup> Chunyan Bao,<sup>b</sup> Zongping Xie,<sup>a</sup> Qiuning Lin<sup>\*b</sup> and Linyong Zhu<sup>b</sup>

The regeneration of articular cartilage, which scarcely shows innate self-healing ability, is a great challenge in clinical treatment. Stem cell-derived exosomes (SC-Exos), an important type of extracellular nanovesicle, exhibit great potential for cartilage regeneration to replace stem cell-based therapy. Cartilage regeneration often takes a relatively long time and there is currently no effective administration method to durably retain exosomes at cartilage defect sites to effectively exert their reparative effect. Therefore, in this study, we exploited a photoinduced imine crosslinking hydrogel glue, which presents excellent operation ability, biocompatibility and most importantly, cartilage-integration, as an exosome scaffold to prepare an acellular tissue patch (EHG) for cartilage regeneration. It was found that EHG can retain SC-Exos and positively regulate both chondrocytes and hBMSCs *in vitro*. Furthermore, EHG can integrate with native cartilage matrix and promote cell deposition at cartilage defect sites, finally resulting in the promotion of cartilage defect repair. The EHG tissue patch therefore provides a novel, cell-free scaffold material for wound repair.

Received 16th January 2017,  
Accepted 3rd March 2017

DOI: 10.1039/c7nr00352h

rsc.li/nanoscale

## Introduction

Articular cartilage is an avascular tissue composed of a highly dense matrix with sparse chondrocytes. It shows limited self-healing ability and suffers in harsh biomechanical environments.<sup>1,2</sup> Achieving ideal repair of articular cartilage lesions, which requires the regenerated tissue to exhibit similar composition (hyaline cartilage) and good integration with surrounding cartilage, is one of the most challenging tasks for clinical treatment. Although traditional clinic therapies such as auto-grafting, microfracture and autologous chondrocyte implan-

tation (ACI) can temporarily lead to therapeutic effects, treatment often fails over long time spans because of the fibrosis and poor native tissue integration of cambium.<sup>3</sup>

Over the past few years, therapies based on stem cells have arisen as very promising approaches to cartilage regeneration because of the chondrogenic ability of stem cells.<sup>4–6</sup> Clinical trials have shown that stem cell based therapies obtain comparable healing results to ACI, but the treatment procedure is simpler and more economical.<sup>7</sup> However, stem cells often show abnormalities in cell phenotype, differentiation and proliferation ability when cultured *in vitro* after many passages or extracted from aged or diseased donors.<sup>8,9</sup> Undesired hypertrophy and ossification of newly formed tissue can also be observed in stem cell based cartilage regeneration.<sup>10,11</sup> In recent years, increasing numbers of research efforts have demonstrated that rather than direct differentiation into the target tissue, transplanted stem cells are more likely to exert their function in a paracrine manner, especially by secreting extracellular vesicles.<sup>12–15</sup> As the most prominent extracellular vesicles that respond to cell–cell communication and cellular immunity, exosomes are nano-sized (30–100 nm) and contain various types of nucleic acids and proteins.<sup>16–18</sup> Analogous to stem cell based therapies, investigations have corroborated the promotional effect of stem cell-derived exosomes on tissue repair and regeneration, and it is believed that the exosome inclusions induce epigenetic changes in recipient cells and

<sup>a</sup>Institute of Microsurgery on Extremities, Department of Orthopaedic Surgery, Shanghai Jiaotong University Affiliated Sixth People's Hospital, 600# Yishan Road, Shanghai, China, 200233. E-mail: wangyang63@sju.edu.cn; Fax: +86-21-64363802; Tel: +86-21-24056319

<sup>b</sup>Key Laboratory for Advanced Materials, Institute of Fine Chemicals, East China University of Science and Technology, 130# Meilong Road, Shanghai, 200237, China. E-mail: qiuninglin@ecust.edu.cn; Fax: +86-21-64253742; Tel: +86-21-64253950

†Electronic supplementary information (ESI) available: Positive regulation of hiPSCs-MSCs-derived exosomes on the proliferation and migration of plate-cultured chondrocytes and hBMSCs, image of rabbit articular cartilage defect filled with *in situ* formed EHG, statistical data of cell densities at the articular cartilage defect treated with *in situ* formed EHG or HG, OCT image of normal rabbit hind leg joint, image of H&E staining and immunohistochemical staining, ICRS II scoring data. See DOI: 10.1039/c7nr00352h

‡These authors contributed equally to this work.

positively regulate their fates such as the promotion of proliferation or the inhibition of apoptosis.<sup>19–27</sup> Besides, the utilization of non-self-reproducible SC-Exos avoids the safety concern of direct cell transplantation. Meanwhile, SC-Exos are more easily manufactured, handled, characterized and stored than stem cells. Therefore, SC-Exos show great potential as acellular factors for articular cartilage regeneration to replace stem cell-based therapy.

Currently, the common mode of administration of SC-Exos is *via* injection, which is not very effective because it is difficult for SC-Exos to be retained at the cartilage defect site, and rapid clearance inevitably occurs. Regeneration of cartilage lesions often takes a relatively long time, and it is necessary to achieve effective retention of SC-Exos at cartilage defect sites to durably exert their function. In order to realize ideal cartilage defect repair, local injection has to be conducted every week during the healing process, which complicates the exosome application and increases pain for the hosts.<sup>25</sup> Embedding exosomes in a hydrogel tissue patch will therefore provide a feasible solution to effectively retain exosomes at cartilage defects. Hydrogel materials have been widely used as cell or factor scaffolds for cartilage regeneration to better fill the cartilage defect and provide a mode for cartilage regeneration, due to their unique features (*i.e.* high water content, swelling behavior, biocompatibility, modulated 3D networks and high cartilage matrix mimetics).<sup>28,29</sup> To date, only a few works have been reported that use hydrogel tissue patches as exosome scaffolds for cartilage regeneration. An ideal hydrogel tissue patch to ensure SC-Exos function in the repair and regeneration of cartilage defect requires the following: (1) *in situ* gelling on the cartilage defect to achieve an accurate fit with irregularly shaped tissue defects; (2) effective retention of SC-Exos at the cartilage defect site; (3) seamless hydrogel-cartilage integration, which significantly facilitates the migration of circumjacent cells into the hydrogel scaffold as well as the SC-Exos nest. Based on the above, once cells migrate into the SC-Exos encapsulating hydrogel, exosomes can be internalized and exert their positive regulation on cells to durably guide cartilage repair and regeneration. However, most of the current hydrogel scaffold materials cannot satisfy the above requirements. Very recently, a novel hydrogel glue, the photoinduced imine crosslinking (PIC) hydrogel, was developed, in which *o*-nitrobenzyl alcohol moieties modified hyaluronic acids (HA-NB) generate aldehyde groups under light irradiation and subsequently react with amino groups distributed on other polymers (*e.g.* chitosan, gelatin) or on tissue surfaces to form a hydrogel *in situ* and simultaneously realize seamless hydrogel-tissue attachment and integration.<sup>30,31</sup> The remarkable operability, biocompatibility, tissue adhesive and integration ability of PIC hydrogel glue made it quite suitable as an SC-Exos scaffold for cartilage defect repair. Hence, we report herein the encapsulation of SC-Exos into the PIC hydrogel glue to prepare a SC-Exos complexed hydrogel tissue patch (Fig. 1). We anticipate that through combining the positively reparative effect of SC-Exos and the advanced features of PIC hydrogel glue, our strategy will provide a more effective scaffold to

promote the repair and regeneration of articular cartilage defects.

## Materials and methods

### Preparation of stem cell-derived exosomes

**Induction and culture of hiPSC-derived MSCs.** Human induced pluripotent stem cell line (iPS-S-01) was provided by the Institute of Biochemistry and Cell Biology of the Chinese Academy of Sciences. hiPSC-MSCs were induced and cultured according to a previous report.<sup>23</sup> Briefly, hiPSCs were expanded on human ESC-Qualified BD Matrigel (BD Biosciences®, Sparks, MD, USA) in standardized mTeSR1 medium (StemCell Technologies®, Vancouver, BC, Canada). Then, mTeSR1 medium was replaced with MSC medium that was composed of Dulbecco's Modified Eagle Medium (DMEM) – low glucose (Corning®, Tewksbury, MA, USA) supplemented with 10% fetal bovine serum (FBS) and 2 mM L-glutamine (Gibco®, Grand Island, NY, USA), and cultured for 14 days. The cells were then trypsinized (0.25% trypsin/mM EDTA, Gibco®) and reseeded in 0.1% gelatin-coated cell culture flasks (Corning®) in MSC medium until passage 4. The induced cells were maintained in MSC medium and cultured at 37 °C with 5% CO<sub>2</sub>.

**Isolation and purification of hiPSC-MSCs-derived exosomes.** After reaching 80% confluency in a 75 cm<sup>2</sup> cell culture dish, hiPSC-MSCs were rinsed three times with phosphate buffered saline (PBS) and cultured with MesenGro® Chemically Defined medium (StemRD®, San Francisco, CA, USA) for 48 h. Exosomes secreted by the cells were released into the medium. The above medium was collected for further isolation and purification of exosomes. To remove cellular debris, the obtained medium was centrifuged at 300g for 10 min, 2000g for 10 min at 4 °C, followed by filtering with a 0.22 μm sterilized filter (Millipore®). The supernatant was further ultracentrifuged at 100 000g for 2 h. Exosomes at the bottom of the centrifuge tube were resuspended in PBS, then transferred to the upper compartment of Amicon Ultra-15 Centrifugal Filter Units (Millipore®) and centrifuged at 4000g at 4 °C until the volume in the upper compartment was reduced to approximately 200 μL.

**Characterization of hiPSC-MSCs-derived exosomes.** The size and concentration of hiPSC-MSCs-derived exosomes were measured using the qNano platform (Izon® Science, UK). The detection technique of the qNANO platform is based on Tunable Resistive Pulse Sensing (TRPS), which allows high-throughput single particle measurement as these particles are driven through the size-tunable nanopores of the facility. A temporary decrease in current is detected when particles pass through the nanopores, allowing for the sizing and counting of particles in electrolyte solution. Firstly, the NP100 nanopores of the measuring system are calibrated using particles of known size (CPC100 standard solutions, IZON® Science), then washed 3 times with PBS. The samples of hiPSC-MSCs-derived exosomes were diluted with 1000-fold PBS and then added to

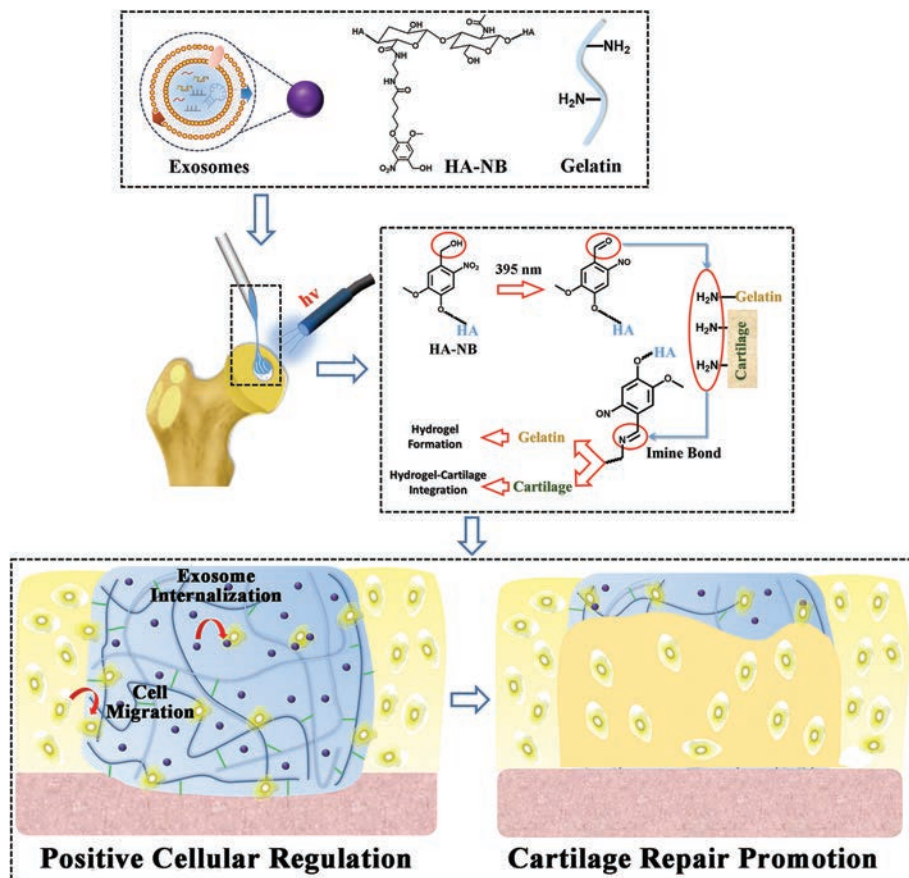


Fig. 1 Schematic illustration of the EHG tissue patch for cartilage regeneration.

the nanopores for measurement. Particle size measurement and data analysis were performed with a particle analyzer (qNano platform, iZON® Science) and Control Suite software v2.2 (iZON® Science). The morphology of hiPSC-MSCs-derived exosomes was observed by TEM. The suspension of hiPSC-MSCs-derived exosomes was dropped on the copper grid and dried in the air. Then, the sample was fixed with 3% glutaraldehyde for 2 h and washed with PBS, followed by negative staining with 2% uranyl acetate for 30 seconds. The morphology of the exosomes was observed using TEM (Hitachi®, Tokyo, Japan) and the images were captured using a digital camera (Olympus®, Tokyo, Japan). Specific markers of hiPSC-MSCs-derived exosomes (CD9, CD63, CD81) were tested by western blotting. hiPSC-MSCs-derived exosomes were treated with protein loading buffer and heated at 95 °C for 5 min, followed by loading to 12% SDS-PAGE polyacrylamide gels at 120 V for 45 min. After that, the loaded samples were transferred to nitrocellulose membranes (Whatman®, Maidstone, Kent, UK) at 100 mA for 1.5 h. The membranes were incubated with primary rabbit polyclonal antibodies (Abcam®, Cambridge, UK) at 4 °C overnight. After washing three times with tris-buffered saline containing tween (TBST), the membranes were incubated with horseradish peroxidase-conjugated goat anti-rabbit secondary antibody (Abcam®) at

37 °C for 1 h, then washed three times with TBST. The proteins were detected with enhanced chemiluminescence (Thermo®) and imaged by Image Quant LAS 4000 mini bio-molecular imager (GE Healthcare®, Uppsala, Sweden).

#### Preparation and characterization of EHG

**Preparation of EHG.** HA-NB was synthesized according to previous reports, with NB grafting ratio of 8%.<sup>30</sup> Gelatin was purchased from Sigma Aldrich. First, HA-NB and GL were accurately weighed and added into sterilized tubes, followed by adding a certain amount of DPBS. The mixture was shaken at 37 °C until the polymer contents were totally dissolved. Then, the solution was adjusted to pH = 7.4 by NaOH aqueous solution and sterilized with a 0.22 μm membrane (Millipore®) to get the HG precursor solution. Thereafter, medium containing hiPSC-MSCs-derived exosomes was mixed with the above solution to obtain the EHG precursor solution (content of HA-NB and GL was 50 mg mL<sup>-1</sup> with the mass ratio of 1 : 1). Finally, the EHG precursor solution was irradiated with 395 nm LED light (20 mW cm<sup>-2</sup>) to prepare the EHG tissue patch.

**Rheological properties of the EHG tissue patch.** The rheological properties of the EHG tissue patch precursor solution were tested using a HAAKE MAS III Rheometer (Thermo Fischer®, Germany) equipped with parallel-plate (P20 TiL,

20 mm diameter) geometry and OmiCure® Series 2000 light source. The EHG precursor solution (200  $\mu\text{L}$ ) was added to the parallel-plate geometry at 37 °C. Time-sweep oscillatory tests were performed at a 10% strain, 1 Hz frequency and a 0.5 mm gap (CD mode) for 300 s. Strain sweeps were performed on the hydrogel precursor solution to verify the linear response. The gel time was determined as the time when the storage modulus ( $G'$ ) surpassed the loss modulus ( $G''$ ).

#### Internalization of hiPSC-MSCs-derived exosomes by encapsulated chondrocytes

hiPSC-MSCs-derived exosomes were harvested and suspended at a density of  $1 \times 10^{12} \text{ mL}^{-1}$  in MesenGro Chemically Defined Medium (StemRD®, San Francisco, CA, USA), followed by fluorescence labeling with DiI Cell-Labeling Solution (Invitrogen®, Carlsbad, CA, USA) as the manufacturer's protocol. The medium containing DiI-labeled exosomes was blended with HG precursor solution and chondrocyte suspension ( $1 \times 10^5 \text{ mL}^{-1}$ ) and then 200  $\mu\text{L}$  of mixture solution was irradiated to form the EHG tissue patch with chondrocyte encapsulation. After being placed in DMEM with 10% FBS at 37 °C and 5%  $\text{CO}_2$  for 24 h, the hydrogel patch was placed in 400  $\text{U mL}^{-1}$  type II collagenase for 24 h, then the encapsulated chondrocytes were centrifuged to separate them from uninternalized exosomes and re-seeded on the plate followed by fixation with paraformaldehyde, DAPI staining and microscopic observation.

#### The exosome retention ability of the EHG tissue patch

The exosome retention ability of the EHG tissue patch was also tested using a particle analyzer (qNano platform, iZone® Science). Briefly, the exosome suspension was mixed with HG precursor solution to approach a final exosome concentration of  $2.45 \times 10^{12}$ , then 200  $\mu\text{L}$  of prepared EHG were placed in cell culture wells of a 48-well plate with 200  $\mu\text{L}$  PBS; the PBS was collected daily and replaced with 200  $\mu\text{L}$  fresh PBS. The amount of leaching exosomes in the collected PBS was detected on a qNANO platform as described above and the retained amount of exosomes were calculated by the total amount of exosomes minus the amount of leaching exosomes.

#### Positive cellular regulation of the hiPSCs-MSCs-derived exosomes

**Plate-cultured cell migration and proliferation test.** The cell migration assay was performed using a scratch assay. Briefly, hBMSCs and chondrocytes were respectively seeded into a 12-well plate with a density of  $5 \times 10^4$  cells per well and cultured until 100% confluence. Two parallel scratches were made with a 200  $\mu\text{L}$  pipette tip in each well and the width of the scratch was measured as the baseline. The cells were then replaced with culture medium containing different concentrations of exosomes ( $1 \times 10^{10}$ ,  $1 \times 10^{11} \text{ mL}^{-1}$ ) or with culture medium for 8 and 12 h. The width of the scratch was measured by mimicking an exclusion zone assay using ImageJ software, and visualized with a light microscope (Leica®, Germany). For the proliferation assay, hBMSCs and chondro-

cytes were respectively seeded into a 96-well plate with a density of  $4 \times 10^3$  cells per well and allowed to attach for 4 h. Then, each well was replaced with culture medium containing different concentrations of exosomes (0,  $1 \times 10^{10}$ ,  $1 \times 10^{11}$ ,  $1 \times 10^{12} \text{ mL}^{-1}$ ), and cells were incubated with these media for 5 d. After that, 10  $\mu\text{L}$  of CCK-8 solution was added into each well and incubated for 3 h. The absorbance value at 450 nm was detected using a microplate reader (Bio-Rad®, Berkeley, CA, USA). The medium was changed every day after observation.

**Encapsulated cell viability.** Suspensions of chondrocytes or hBMSCs were mixed with hydrogel precursor solution (50  $\text{mg mL}^{-1}$  HA-NB and GL, mass ratio 1 : 1) with or without exosomes at a density of  $1 \times 10^5 \text{ mL}^{-1}$ . Then, 200  $\mu\text{L}$  of mixture solution was added to the bottom of 48-well plates, followed by 395 nm light irradiation to encapsulate cells in the hydrogel. At 0, 1 and 3 days, live/dead staining agents were added to each and the cell viability was visualized using fluorescence microscopy. The cell viability was calculated by counting the amount of live cells in each well, using ImageJ.

#### *In vivo* promotion effect of EHG on cell deposition at cartilage defects

In order to examine the *in vivo* proliferation and migration proliferation effect of EHG, the rabbit articular cartilage defect model was exploited and all animal experiments in the paper were approved by the Animal Research Committee of the Sixth People's Hospital at Shanghai Jiao Tong University. Six New Zealand rabbits weighing 2.5–3.0 kg were randomly divided into 2 groups. A lateral *para*-patellar skin incision was made in each joint of the rabbits and the joints were exposed after medial dislocation of the patella. A full – thickness cylindrical osteochondral defect of 4 mm in diameter and 3 mm in depth was created in the patellar groove using a stainless steel drill. Thereafter, the defect sites in the rabbits of both groups were respectively filled with 20  $\mu\text{L}$  precursor solution of EHG tissue patch or HG, followed by 1 min of 395 nm LED light irradiation (20  $\text{mW cm}^{-2}$ ). On the seventh day after surgery, all the rabbits were sacrificed by injecting an overdose of anesthetic and the knees of each rabbit were collected. Finally, after standard procedures of tissue fixation, the defect sites were visualized by H&E staining and DAPI staining. The cell densities at the defect sites were determined using ImageJ.

#### *In vivo* cartilage defect repair and regeneration

To evaluate the promotional effect of EHG on the repair and regeneration of cartilage defect, the rabbit articular cartilage defect model was also exploited and the surgery procedure was the same as mentioned above. Twenty New Zealand rabbits weighing 2.5–3.0 kg were randomly divided into 5 groups, in which the defect sites were respectively treated with (1) 20  $\mu\text{L}$  *in situ* formed EHG containing  $1 \times 10^{11} \text{ mL}^{-1}$  hiPSC-MSCs-derived exosomes (EHG); (2) 20  $\mu\text{L}$  *in situ* formed HG (HG); (3) implantation of 20  $\mu\text{L}$  *in vitro* preformed EHG containing  $1 \times 10^{11} \text{ mL}^{-1}$  exosomes (Pre-EHG); (4) intra-articular injection of a 20  $\mu\text{L}$  exosome suspension with exosome concentration of  $1 \times 10^{11} \text{ mL}^{-1}$  (Inj-Exos); (5) saline rinsing (Cont). Twelve

weeks later, all the rabbits were sacrificed with an overdose of anesthesia and the joints of each rabbit were harvested for further evaluation. First, the gross appearance of each sample was scored according to the ICRS macroscopic scoring system and recorded by camera. In addition, the samples were also evaluated using OCT imaging (HSL-2100, Santec®, Japan). The test parameters were as follows: wavelength ( $\lambda$ ) 1315–1340 nm, output power 20–30 mW, scanning frequency 20 kHz and distance of 60 mm. The samples were decalcified with 10% EDTA, then dehydrated through a series of graded alcohols, embedded in paraffin and sectioned at 8  $\mu$ m thickness. Sections were stained with hematoxylin & eosin and safranin O/fast green. For immunohistochemistry, sections were blocked with 1% BSA (Gibco®) for 1 h at room temperature, then incubated in the primary antibodies (collagen type I, collagen type II; mouse clone, 1 : 200; Merck®) at 4 °C overnight. Following 3 washes in PBS, the sections were incubated with the secondary antibodies for 1 h at room temperature. Finally, the sections were stained in diaminobenzidine solution with hematoxylin counterstaining. The sections were observed using a light microscope (Leica®, Germany). The repairing effects were evaluated by ICRS recommended guidelines.<sup>32</sup>

### Statistical analysis

The numerical data in the study were presented as mean  $\pm$  standard deviation (s.d.) and one-way ANOVA was exploited to evaluate the statistical difference among groups and  $p < 0.05$  was considered to be a significant difference.

## Results and discussion

### Extraction of SC-Exos and preparation of SC-Exos complexed PIC hydrogel glue

In this study, exosomes extracted from human induced pluripotent stem cells (hiPSCs) derived mesenchymal stem cells (MSCs) were used because of the infinite extension ability of hiPSCs, making it probable to produce sufficient amounts of exosomes for practical application. The exosomes were extracted from the culture medium of hiPSCs derived MSCs by multiple centrifugation. As shown in Fig. 2a, the main size distribution of the extracted vesicles were in the range of 50–150 nm, generally corresponding to the exosome size distribution in other reports.<sup>33,34</sup> From the TEM image (Fig. 2b), the vesicles with the size of 30–60 nm that exhibited spherical morphology were clearly observed, indicating the presence of exosomes. Furthermore, the western blotting results (Fig. 2c and S1†) showed the expression of exosome markers such as CD9, CD63 and CD81. All the above results demonstrated that we had successfully extracted exosomes from hiPSCs derived MSCs.

Next, we chose the PIC hydrogel glue that was composed of HA-NB and gelatin (GL) as the scaffold materials for both exosomes and cells. We blended the exosome medium with the precursor solution of the hydrogel glue, followed by light irradiation (395 nm, 20 mW  $\text{cm}^{-2}$ ) to prepare the SC-Exos

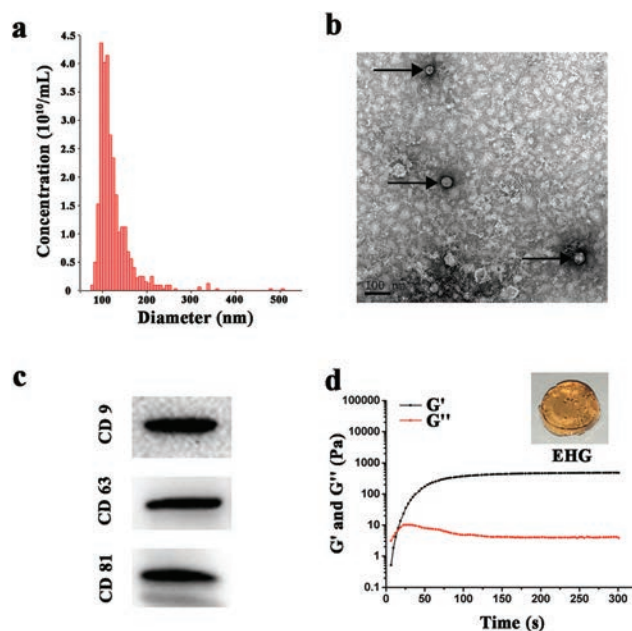


**Fig. 2** Characterization of the extracted exosomes and the EHG. (a) Size distribution of exosomes extracted from hiPSCs derived MSCs by nanoparticle analyzer (qNano platform, IZon®). (b) TEM image of the extracted exosomes, scale bar: 100 nm. (c) Western blotting analysis of the surface markers of the exosomes, which showed the clear existence of CD9, CD63 and CD81. (d) Dynamic rheological properties of the EHG precursor solution under light irradiation (OmniCure®, S2000, 70% output power) using HAAKE MAS III rheometer (CD mode,  $f = 1$  Hz,  $\gamma = 10\%$ , gap = 0.5 mm).

encapsulating hydrogel glue tissue patch – EHG (polymer content of 50  $\text{mg mL}^{-1}$  and HA-NB:GL mass ratio of 1 : 1). The rheological properties of the EHG precursor solution are shown in Fig. 2d, from which it is obvious that the EHG precursor solution could gel in 20 s under light irradiation, forming a stable 3D structure.

### Exosome retention ability and positive cellular regulation of EHG

After successfully preparing the EHG tissue patch, we tested whether our hydrogel could effectively retain exosomes inside. EHG (200  $\mu$ L) with exosome concentration of  $2.45 \times 10^{12} \text{ mL}^{-1}$  was immersed in 200  $\mu$ L PBS, and was refreshed with the same amount of PBS every day. The exosome content in the PBS collected everyday was detected by particle analyzer (qNano platform, IZon® Science). As shown in Fig. 3a, it was obvious that most of the encapsulated exosomes were retained inside the hydrogel (>90%) after immersing in PBS for 14 days. This result indicated that EHG could effectively retain exosomes inside the hydrogel. According to the classical rubber theory, the theoretical mesh size of the EHG hydrogel was about 25 nm, which was smaller than the size of exosomes; thus, the majority of the exosomes were retained inside the EHG tissue patch. In addition, according to the results, more than  $1 \times 10^{10} \text{ mL}^{-1}$  exosomes were released every day, which had the potential to show positive regulation to the surrounding cells. We

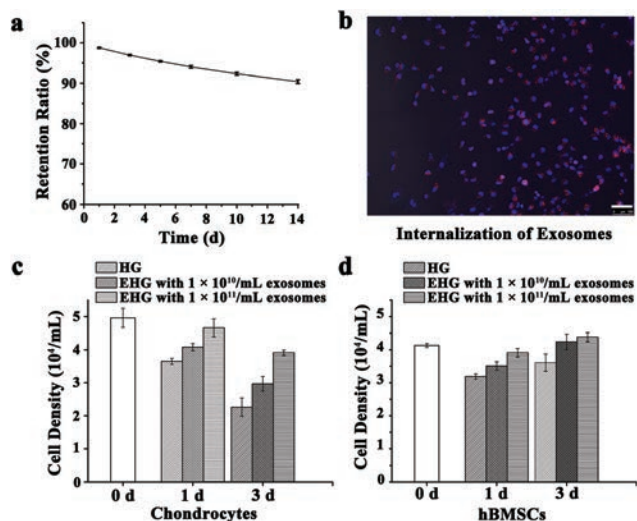


**Fig. 3** Exosome retention ability of EHG and its positive cellular regulation. (a) The exosome retention ratio of the EHG tissue patch after immersing in PBS for 14 days. The data were tested using a particle analyzer (qNano platform, IZon®). (b) Internalization of Dil-labeled exosomes in EHG by encapsulated chondrocytes: chondrocytes were firstly encapsulated in the Dil-labeled-EHG for 24 h, after which EHG was degraded by 400 U mL<sup>-1</sup> type II collagenase and the encapsulated chondrocytes were separated and re-seeded on plates, followed by fixation and DAPI staining; scale bar: 100 μm. The live cell density of chondrocytes (c) and hBMSCs (d) encapsulated in EHG or HG for 1 day and 3 days.

thought this property was very important for the EHG as an effective acellular scaffold for cartilage defect regeneration, because the exosomes could be retained at the defect site and had the potential to effectively and durably exert their positive regulation on both the surrounding and migrated cells, resulting in the promotion of cartilage defect repair.

It is well known that SC-Exos positively impact cells through transporting their cargos. Thus, we investigated whether exosomes inside EHG could be internalized by encapsulated cells. hiPSCs-MSCs-derived exosomes were labeled with a lipophilic fluorescent dye, 1,1'-dioctadecyl-3,3,3',3'-tetramethylindocarbocyanine (DiI), before blending with the hydrogel precursor solution containing HA-NB and GL. Then, 1 × 10<sup>5</sup> per mL cells were encapsulated in the DiI-labeled-EHG. Twenty four hours later, the hydrogel was degraded by collagenase, after which the encapsulated chondrocytes were centrifuged to separate them from nomadic exosomes. As shown in the fluorescence microscope image (Fig. 3b and S2†), the red fluorescence of DiI-labeled exosomes was clearly observed in the cytoplasm of the chondrocytes, suggesting the successful endocytosis of exosomes by encapsulated cells in EHG. In order to investigate whether our extracted SC-Exos could exhibit positive regulation on cells, plate-cultured chondrocytes and human bone marrow stem cells (hBMSCs), both of which were the most important cell types for cartilage regeneration, were incubated with the medium containing different concentrations of exosomes. As shown in Fig. S3,† it was con-

firmed that the extracted hiPSCs-MSCs-derived exosomes could promote the migration and proliferation of plate-cultured chondrocytes and hBMSCs, implying their positive regulation effects. Thereafter, we encapsulated chondrocytes and hBMSCs in EHG tissue patch or hydrogel without exosomes (HG), followed by 3D cell culturing for 3 days. The everyday viability of encapsulated cells was tested *via* live/dead staining and cell counting. As shown in Fig. 3c and d, although having the same initial live cell density, the live cell density of encapsulated cells in EHG was significantly larger than that of HA-NB/GL hydrogel (HG) without exosomes at 1 d and 3 d, and with increasing exosome concentration, this trend was more obvious. This result showed that EHG could maintain the viability of encapsulated chondrocytes and hBMSCs, demonstrating its positive cellular regulation for cartilage repair. Overall, the above results indicate that the EHG could effectively retain exosomes and positively regulate chondrocytes and hBMSCs, all of which make it quite suitable as a scaffold to promote the repair and regeneration of cartilage defects.

#### Seamless cartilage-integration ability of EHG and its positive impact on cell deposition at cartilage defects *in vivo*

The cartilage integration ability of the EHG tissue patch is a very important factor for cartilage regeneration. The seamless cartilage integration could facilitate the surrounding cell migration into the EHG scaffolds, after which SC-Exos could exert their positive cellular regulation. In addition, previous reports have demonstrated that with lack of cartilage integration ability, cartilage regeneration failure could happen when using scaffold materials.<sup>35,36</sup> Considering the unique gelling mechanism, EHG could form chemical bonds with the cartilage matrix, thus leading to seamless cartilage integration. Therefore, we examined the interface between our hydrogel and the cartilage surface by filling a full-thickness defect in the knee of a rabbit's hind leg with an *in situ* formed EHG tissue patch (Fig. S4†). The interface between the hydrogel and cartilage was visualized by SEM observation and H&E staining and as shown in Fig. 4a, a clear and seamless interface was observed between them under SEM observation. Furthermore, as shown in the H&E staining image (Fig. 4b), it was found that the formed hydrogel was fully attached to the lateral cartilage, even after the decalcification and fixation process of the sectioned sample, and the seamless interface still existed between cartilage and hydrogel. This result proved the stable attachment between EHG and cartilage. In addition, the EHG hydrogel also penetrated into the subchondral bone and formed a seamless interface. This property may facilitate the penetration of MSCs from beneath tissues into the hydrogel. All the above results demonstrated the cartilage integration ability of EHG, which laid its foundation for intravital cartilage repair.

The full-thickness defect model of rabbit articular cartilage was then exploited to demonstrate the positive regulation of EHG on cartilage regeneration *in vivo*. A full-thickness articular cartilage defect with diameter of 4 mm was made on each

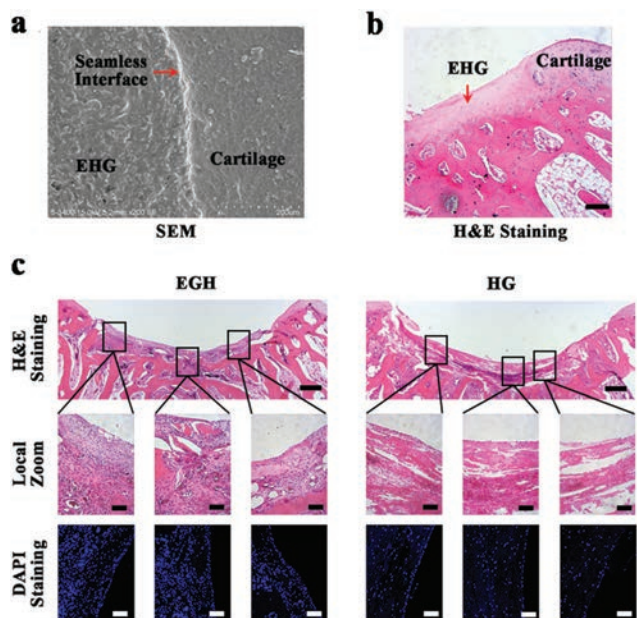


**Fig. 4** The seamless and tight integration of EHG with cartilage defect: (a) SEM image of the seamless interface between cartilage and EHG tissue patch; (b) H&E staining image of the sectioned samples, scale bar: 250  $\mu\text{m}$ . (c) *In vivo* promotion of the EHG tissue patch on cell deposition at the defect sites: H&E and DAPI staining images from the articular defect sites that were respectively treated with EHG or HG; scale bars from (a) to (c) were 500  $\mu\text{m}$ , 100  $\mu\text{m}$  and 50  $\mu\text{m}$ , respectively.

hind leg joint of New Zealand rabbits. These defects were respectively treated with 20  $\mu\text{L}$  of *in situ* formed EHG tissue patch, or mere HG without exosomes. Seven days after surgery, the defect joints treated with *in situ* formed EHG or HG were harvested and observed using H&E and DAPI staining. As shown in Fig. 4c and S5,<sup>†</sup> the cell populations of the defect sites treated with EHG were significantly larger than those of the defect sites treated with HG. From cell morphology observations, the deposited cells probably included chondrocytes, inflammation cells, fibroblasts and blood cells, all of which are common during the wound healing process. Based on the above, the seamless hydrogel-tissue integration ensured the migration of related cells into the hydrogel and the encapsulated SC-Exos showed positive effects on cells *in vivo* as in the *in vitro* results, both of which could benefit from our acellular hydrogel glue scaffold on cartilage repair.

#### ***In vivo* evaluation of the EHG therapeutic effect on cartilage defects**

Finally, we examined the ultimate reparative effect of the EHG tissue patch on cartilage defect repair. The surgery procedure was the same as mentioned above. In addition to the experiment group in which the defects were treated with the *in situ* formed EHG tissue patch, and the control groups in which the defects were treated with *in situ* formed HG or saline rinsing (Cont), the defect sites that were treated with *in vitro* pre-formed EHG (Pre-EHG) or one time injection of hiPSC-MSCs-

derived exosome suspension (Inj-Exos) were also set as control groups to evaluate the impacts of hydrogel-cartilage integration and exosome administration manner on cartilage defect repair. Twelve weeks after surgery, the whole joints of all rabbits were collected and the cartilage regeneration results were evaluated by gross view examination, optical coherence tomography (OCT) and histological analysis, including H&E staining, safranin-O staining and immunohistochemical staining. As shown in the gross view of the harvested cartilage sample from the experiment group (Fig. 5a1), the glistening white regenerated tissue with smooth surface filled the defect site entirely, as well as integrated with the surrounding cartilage. Furthermore, to observe the repair effects such as surface smoothness and filling more clearly and deeply, OCT was used for the imaging of the harvested samples *in situ*. The OCT imaging result of the experiment group (Fig. 5a2) was similar to that of the normal rabbit joint cross section (Fig. S6<sup>†</sup>), which exhibited a uniform and well-organized articular cartilage structure. From the H&E staining image (Fig. S7a<sup>†</sup>), it was clearly shown that newly formed tissue with many resident chondrocytes completely covered the defect site and was totally integrated with the native cartilage layer. Furthermore, the strong positive staining of safranin-O (Fig. 5a3), as well as type II collagen (Fig. 5a4) and weak type I collagen (Fig. S8a<sup>†</sup>) staining demonstrated that the newly formed tissue was almost hyaline cartilage, which is the same as the native cartilage composition. Collectively, the above results indicate that the EHG tissue patch could achieve ideal articular cartilage regeneration.

However, the reparative results of other groups were much inferior to the experiment group. In the HG group (Fig. 5b1–b4, S7b and S8b<sup>†</sup>), the newly formed tissue was hyaline cartilage and showed integration with native tissue, but was much thinner than that of the experiment group (EHG), implying the promotional effect of hiPSC-MSCs-derived exosomes on tissue regeneration. In the pre-EHG group, we observed obvious clefts between newly formed tissue and native tissue (Fig. 5c1–c4, S7c and S8c<sup>†</sup>). We speculated that this phenomenon may be caused by the gaps between the *in vitro* pre-formed EHG tissue patch and native tissue, which resulted in non-uniform cell migration along the edge of the hydrogel scaffold. Thus, the EHG tissue patch could not fully guide tissue regeneration at certain sites, especially at edge sites, leading to tissue discontinuity. As previously reported, this result further demonstrated that the seamless tissue integration ability is very important for hydrogel scaffolds to guide cartilage repair and regeneration.<sup>35</sup> In addition, similar to the Cont. group, the repair of cartilage defects in the Inj-Exos group also failed, indicating the low efficacy of exosome injection (Fig. 5d1–d4, e1–e4, S7d, S7e, S8d and S8e<sup>†</sup>). Finally, we evaluated the histological scores of the samples from each group based on the recommended guidelines of the International Cartilage Repair Society (ICRS). As shown in Fig. S9,<sup>†</sup> the *in situ* formed EHG tissue patch group gained the highest score among all the groups. Overall, the *in situ* formed EHG tissue patch could accurately fit the cartilage defect and facilitate cell migration

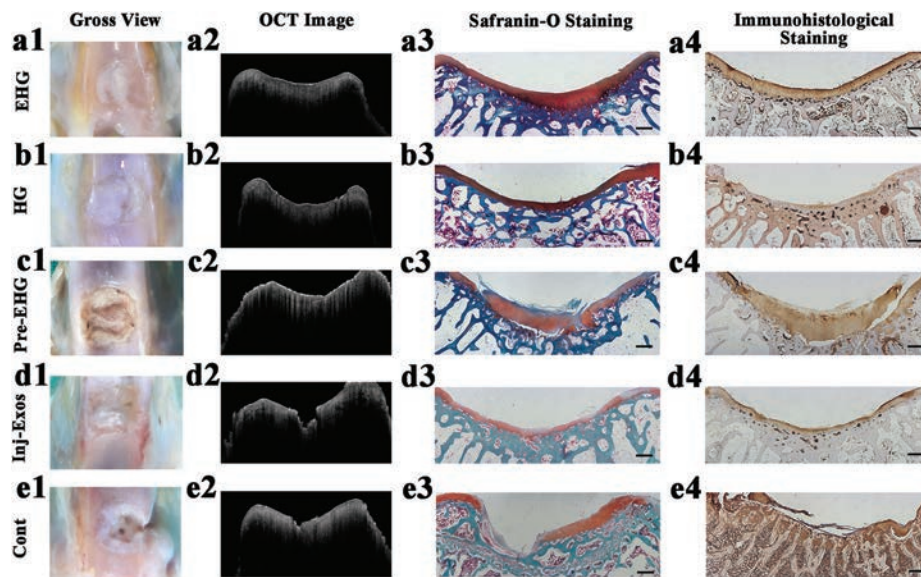


**Fig. 5** The ultimate reparative results of the rabbit articular full-thickness cartilage defects treated by the *in situ* formed EHG tissue patch (EHG), *in situ* formed HG tissue patch (HG), *in vitro* preformed EHG tissue patch (Pre-EHG), one time injection of hiPSC-MSCs-derived exosome suspension ( $1 \times 10^{11} \text{ mL}^{-1}$ , Inj-Exos) and, saline rinsing (Cont). (a1–e1): Gross view image of the regenerated tissues; (a2–e2) OCT view image of the regenerated tissue cross sections; (a3–e3) safranin-O staining image of the regenerated tissues, scale bar: 500  $\mu\text{m}$ ; (a4–e4) immunohistochemical staining of type II collagen of the regenerated tissues, scale bar: 500  $\mu\text{m}$ .

into the scaffold, after which the encapsulated exosomes could exert their positive regulation to promote cell proliferation and corresponding matrix secretion. Thus, the EHG tissue patch guided the integration of newly formed cartilage with native tissue and resulted in the quite successful repair and regeneration of cartilage defects.

Very recently, the Toh group successfully achieved cartilage repair using SC-Exos (embryonic stem cell-derived exosomes); however, the exosome suspension had to be injected into the articular cavity every week, indicating the low effectiveness of local injection.<sup>25</sup> From our results, it was clearly showed that the EHG tissue patch could achieve reparative effect by one time implantation, demonstrating its high effectiveness and this property can drastically reduce the dosage of exosomes. Furthermore, the EHG tissue could also provide a mode for cartilage regeneration and promote integration. In addition, the *in situ* forming ability provides the EHG tissue patch with the potential for combining with the arthroscopic technique. In general, the EHG tissue patch showed better application value for clinical cartilage defect treatment and could promote the practical utilization of SC-Exos in regenerative medicines.

## Conclusion

In summary, we have developed an *in situ* formed acellular hydrogel glue tissue patch EHG through combining SC-Exos with PIC hydrogel glue for cartilage defect repair. It is found that the EHG tissue patch can seamlessly integrate with native cartilage and effectively retain exosomes at defect sites. Furthermore, there is positive cellular regulation both *in vitro*

and *in vivo*, which leads to the promotion of cartilage repair and regeneration. Our SC-Exos encapsulating hydrogel glue tissue patch provides a novel cell-free material with great practical value for the extensive repair of tissues and organs.

## Acknowledgements

This work was financially supported by the National Nature Science Foundation of China (Project no. 81672254, 81572120, 81472152, 21425311, 51403061).

## References

- 1 D. J. Huey, J. C. Hu and K. A. Athanasiou, *Science*, 2012, **338**, 917–921.
- 2 J. Klein, *Science*, 2009, **323**, 47–48.
- 3 E. A. Makris, A. H. Gomoll, K. N. Malizos, J. C. Hu and K. A. Athanasiou, *Nat. Rev. Rheumatol.*, 2015, **11**, 21–34.
- 4 P. Pastides, M. Chimutengwende-Gorden, N. Maffulli and W. Khan, *Osteoarthr. Cartilage*, 2013, **21**, 646–654.
- 5 J. A. Anderson, D. Little, A. P. Toth, C. T. Moorman, B. S. Tucker, M. G. Ciccotti and F. Guilak, *Am. J. Sports Med.*, 2014, **42**, 2253–2261.
- 6 C. Madeira, A. Santhagunam, J. B. Salgueiro and J. M. Cabral, *Trends Biotechnol.*, 2015, **33**, 35–42.
- 7 H. Nejadnik, J. H. Hui, E. P. F. Choong, B. Tai and E. H. Lee, *Am. J. Sports Med.*, 2010, **38**, 1110–1116.
- 8 R. Siddappa, R. Licht, C. Van Blitterswijk and J. Der Boer, *J. Orthop. Res.*, 2007, **25**, 1029–1041.

- 9 B. A. Scruggs, J. A. Semon, X. Zhang, S. Zhang, A. C. Bowles, A. C. Pandey, K. M. Imhof, K. A. Kalueff, J. M. Gimble and B. A. Bunnell, *Stem Cells Transl. Med.*, 2013, **2**, 797–807.
- 10 V. Savkovic, H. Li, J. K. Seon, M. Hacker, S. Franz and J. C. Simon, *Curr. Stem Cell Res. Ther.*, 2014, **9**, 469–488.
- 11 A. Dickhut, K. Pelttari, P. Janicki, W. Wagner, V. Eckstein, M. Egermann and W. Richter, *J. Cell Physiol.*, 2009, **219**, 219–226.
- 12 X. Liang, Y. Zhang, H. F. Tse and Q. Lian, *Cell Transplant.*, 2014, **23**, 1045–1099.
- 13 L. Shen, W. Zeng, Y. X. Wu, C. L. Hou, W. Chen, M. C. Yang and C. H. Zhu, *Cell Transplant.*, 2013, **22**, 1011–1021.
- 14 M. Song, J. Heo, J. Y. Chun, H. S. Bae, J. W. Kang, H. Kang, S. W. Kim, D. M. Shin and M. S. Choo, *Stem Cells Dev.*, 2014, **23**, 654–663.
- 15 M. Z. Ratajczak, M. Kucia, T. Jadczyk, N. J. Greco, W. Wojakowski, M. Tendera and J. Ratajczak, *Leukemia*, 2011, **26**, 1166–1173.
- 16 C. Lee, R. P. Carney, S. Hazari, Z. J. Smith, A. Knudson, C. S. Robertson, K. S. Lam and S. Wachsman-Hogiu, *Nanoscale*, 2015, **7**, 9290–9297.
- 17 W. Jo, J. Kim, J. Yoon, D. Jeong, S. Cho, H. Jeong, Y. J. Yoon, S. C. Kim, Y. S. Gho and J. Park, *Nanoscale*, 2014, **6**, 12056–12064.
- 18 I. Vishnubhatla, R. Corteling, L. Stevanato, C. Hicks and J. Sinden, *J. Circ. Biomarkers*, 2014, **3**, 2.
- 19 R. C. Lai, T. C. Chen and S. K. Lim, *Regener. Med.*, 2011, **6**, 481–492.
- 20 A. Dorronsoro and P. D. Robbins, *Stem Cell Res. Ther.*, 2013, **4**, 39.
- 21 Y. Zhou, H. Xu, W. Xu, B. Wang, H. Wu, Y. Tao, B. Zhang, M. Wang, F. Mao, Y. Yan, S. Gao, H. Gu, W. Zhu and H. Qian, *Stem Cell Res. Ther.*, 2013, **4**, 34.
- 22 C. Y. Tan, R. C. Lai, W. Wong, Y. Y. Dan, S. Lim and H. K. Ho, *Stem Cell Res. Ther.*, 2014, **5**, 76.
- 23 J. Zhang, J. Guan, X. Niu, G. Hu, S. Guo, Q. Li, Z. Xie, C. Zhang and Y. Wang, *J. Transl. Med.*, 2015, **13**, 49.
- 24 Y. Nakamura, S. Miyaki, H. Ishitobi, T. Nakasa, N. Kamei, T. Akimoto, Y. Higashi and M. Ochi, *FEBS Lett.*, 2015, **589**, 1257–1265.
- 25 S. Zhang, W. C. Chu, R. C. Lai, S. K. Lim, J. H. P. Hui and W. S. Toh, *Osteoarthr. Cartilage*, 2016, **24**, 2135–2140.
- 26 X. Qi, J. Zhang, H. Yuan, Z. Xu, Q. Li, X. Niu, B. Hu, Y. Wang and X. Li, *Int. J. Biol. Sci.*, 2016, **12**, 836–849.
- 27 K. Nong, W. Wang, X. Niu, B. Hu, C. Ma, Y. Bai, B. Wu, Y. Wang and K. Ai, *Cytotherapy*, 2016, **18**, 1548–1559.
- 28 C. A. Vilela, C. Correia, J. M. Oliveira, R. A. Sousa, J. Espregueira-Mendes and R. L. Reis, *ACS Biomater. Sci. Eng.*, 2015, **1**, 726–739.
- 29 K. L. Spiller, S. A. Maher and A. M. Lowman, *Tissue Eng., Part B*, 2011, **17**, 281–299.
- 30 Y. Yang, J. Zhang, Z. Liu, Q. Lin, X. Liu, C. Bao, Y. Wang and L. Zhu, *Adv. Mater.*, 2016, **28**, 2724–2730.
- 31 J. Zhang, Y. Yang, Y. Chen, X. Liu, S. Guo, L. Zhu and Y. Wang, *J. Mater. Chem. B*, 2016, **4**, 973–981.
- 32 P. Mainil-Varlet, B. Van Damme, D. Nestic, G. Knutsen, R. Kandel and S. A. Roberts, *Am. J. Sports Med.*, 2010, **38**, 880–890.
- 33 E. Van Der Pol, A. G. Hoekstra, A. Sturk, C. Otto, T. G. Van Leeuwen and R. Nieuwlan, *J. Thromb. Haemostasis*, 2010, **8**, 2596–2607.
- 34 E. Van Der Pol, F. A. W. Coumans, A. E. Grootemaat, C. Gardiner, I. L. Sargent, P. Harris, A. S. Sturk, T. G. Van Leeuwen and R. Nieuwland, *J. Thromb. Haemostasis*, 2014, **12**, 1182–1192.
- 35 D. Wang, S. Varghese, B. Sharma, I. Strehin, S. Fermanian, H. Gorham, D. H. Fairbrother, B. Cascio and J. H. Elisseeff, *Nat. Mater.*, 2007, **6**, 385–392.
- 36 Y. S. Chang, H. O. Gu, M. Kobayashi and M. Oka, *Knee*, 1998, **5**, 205–213.